Modeling of Bulk Current Injection (BCI) Setups for Virtual Automotive IC Tests

Sergey Miropolsky[1)], Stephan Frei[1)], Jörg Frensch[2)]
[1)]Technische Universität Dortmund
[2)]ELMOS Semiconductor AG
Dortmund, Germany
sergey.miropolsky@tu-dortmund.de

Abstract — **The Bulk Current Injection (BCI) method is widely used for RF immunity testing of automotive systems and ICs in electronics industry. During testing detected IC failures may lead to expensive redesigns and cause seriously delays of a product launch. To evaluate the chip immunity in early design stages it is desired to perform virtual tests based on accurate models.**

In this paper an accurate and fast to simulate behavioural model of a BCI injection clamp is presented. The applicability is shown with an RF immunity investigation of a sample DUT. Several different configurations of the BCI test setup with different wire lengths and application-dependent line terminations are analyzed. Specific attention is paid to test setup configurations where supply and ground cables are subject of injection. The common and differential mode disturbances and PCB ground shifts are measured and modeled. The simulations show good correlation to measurements and allow performing RF immunity investigations of the designed DUTs on earlier design stages.

Keywords: Automotive EMC, IC EMC, Bulk Current Injection (BCI), common and differential mode disturbances

I. Introduction

BCI testing is widely used in automotive industry for electronic control unit (ECU) testing. In ISO 11452-4 [1] a complete electronic control unit consisting of PCB, connectors, ICs, and enclosure is placed in a BCI setup and reaction to injected currents is observed. Here the maximum frequency is 400 MHz. As ICs are most the critical components there was the need to conduct also direct BCI tests on IC level. The IEC 62132-3 [2] standard proposes test setup for single ICs. Here the maximum frequency was increased compared to ISO up to 1 GHz.

Many approaches to model BCI injection clamps have been proposed. A first investigation based mainly on coupled inductances is described in [3]. A more precise SPICE circuit model of the BCI probe has been developed in [4, 5]. Measurement data was used to create a behavioural model of the probe. The behaviour of the probe core was described with a second order Lorentz model and implemented in a SPICE circuit model. Aiming at more model simplicity, another research group have proposed a similar approach in [6]. The probe ferrite core was modeled here as a SPICE circuit with two behavioural models of frequency-dependent impedances. The coupling to the wire was modeled with two coupled inductances.

The developed models are well suited for frequency domain analysis. Analysis of IC susceptibility requires time domain models and simulations. IC models are mainly available for the time domain. This means the BCI models must support time domain simulations too. Many circuit simulators support frequency dependent parameters using look up tables or functions. Either convolution methods slow down significantly the simulation speed or special automatic approximations are applied in order to have acceptable simulation times. Several numerical problems might appear here and it is desirable to avoid approximations from the circuit solvers. In this paper a circuit approximation that can be directly implemented with any circuit solver in SPICE or VHDL-AMS language is proposed to handle the frequency dependency of the clamp.

Using the model the injection into cables and a test PCB is investigated. The PCB is not connected to ground except the grounding cable under injection. This is often a requirement of the test specification. A model of this setup configuration is developed and verified by measurements.

II. Injection Clamp Modeling

A. *Injection clamp modeling*

The approach implemented here initially is similar to [4], [5], and [6]. All investigations were done with a Fischer FCC F140 BCI-clamp. The input impedance of the injection clamp was measured in absence of the secondary winding. An initial equivalent circuit model was developed to fit the measured input impedance, both real and imaginary parts.

The frequency dependence of the primary winding inductance was extracted from measured input impedance assuming the simple relation:

$$Z(\omega) = j \cdot \omega \cdot L(\omega) \quad (1)$$

These extracted values of the inductance are valid only up to approx. 200 MHz. At higher frequencies the input impedance is determined mostly by input connector and internal parasitics. However, it is sufficient to fit the model parameters. Similarly to [4, 5], the second order Lorentz model of ferrite permeability was used to fit this dependence.

$$\mu(s) = 1 + \frac{A \cdot \omega_0^2}{s^2 + s \cdot \Delta\omega + \omega_0^2}\ ; \quad L(s) = L_0 \cdot \mu(s) \quad (2,3)$$

In the impedance representation the fitting was acceptable, but in the inductance representation the dependency couldn't be fitted with a single model. There had to be two components within this inductance, each described by the same model, but with another set of parameters. This probably corresponds to two serial physical parts in the RF signal path.

By implementing two models serially (see fig. 1) and fitting the parameters, a good correlation with measurements could be achieved in the frequency range up to 100 MHz. By considering also the connector with and equivalent circuit the probe impedance at higher frequencies could be fitted very well above 3 MHz (see fig. 3).

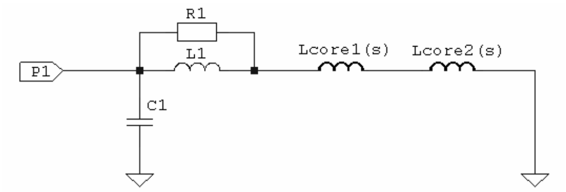

Figure 1. First model of BCI clamp primary winding and input connector

The impedance of such an inductance, where the magnetic permeability frequency dependence is described with Lorentz model, can be written as:

$$Z_L(s) = j\omega \cdot L_0 \cdot \mu(s) = j\omega L_0 + \frac{j\omega L_0 \cdot A \cdot \omega_0^2}{s^2 + s \cdot \Delta\omega + \omega_0^2} \quad (4)$$

where L_0 is the geometrical factor, i.e. the inductance value that would be measured if the ferrite core has unity permeability, under the condition that flux distribution remains unaltered. This is equivalent to the following passive structure:

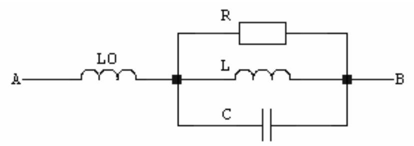

Figure 2. Equivalent circuit model for an inductor with frequency-dependent permeability of the ferrite core

where the component values have the following relations with Lorentz model parameters:

$$\omega_0^2 = \frac{1}{L \cdot C}; \quad \Delta\omega = \frac{1}{R \cdot C}; \quad A = \frac{L}{L_0} \qquad (5\text{-}7)$$

The primary winding inductance was implemented into the clamp model using this equivalent circuit representation.

The input RF connector of a clamp was implemented into the model with a number of LC elements. To extract the component values, a parameter optimization algorithm in Matlab was used. The values were optimized to fit the reflection and impedance curves in the frequency range higher than 200 MHz (see fig. 4).

In the resulting model of the primary winding an acceptable correlation of measurements to simulation was obtained up to the frequency of 1 GHz.

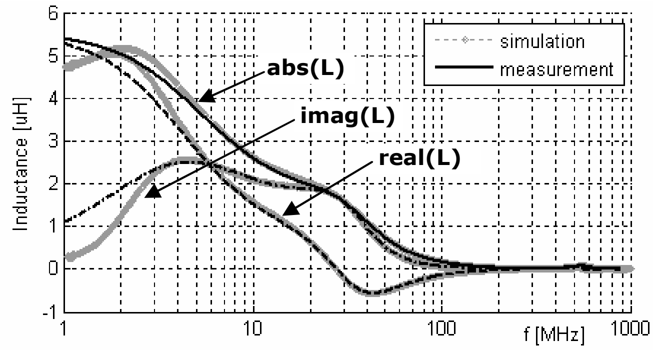

Figure 3. Primary winding inductance of the injection clamp

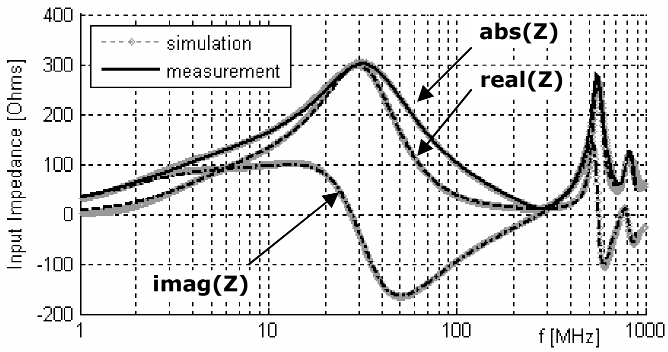

Figure 4. Input impedance of the injection clamp in absence of a secondary winding

B. *Coupling to cables modeling*

To avoid implementation of the same inductance with frequency dependence in the secondary winding, an approach similar to [4, 5] was used. Inductive coupling can be described with the following equations:

$$\begin{aligned} V_1 &= j\omega L_1(\omega) \cdot I_1 + j\omega M(\omega) \cdot I_2 \\ V_2 &= j\omega L_2(\omega) \cdot I_2 + j\omega M(\omega) \cdot I_1 \end{aligned} \qquad (8,9)$$

Assuming that L_1 and L_2 are the windings of the same magnetic core, the equations are transformable to:

$$V_2 = \frac{N_2}{N_1} V_1; \quad I_1 = I_{1L} - I_{1C} = \frac{V_1}{j\omega \cdot L_1(s)} - \frac{N_2}{N_1} I_2 \quad (10,11)$$

where N1 and N2 are the numbers of turns in the windings. This can be implemented in a circuit simulator as following. The secondary winding is represented by a single linear controlled voltage source (V_2). The first winding consists of a primary winding inductance $L_1(s)$ (I_{1L} in eq. 7) and a parallel linear controlled current source (I_{1C} in eq. 7), which reduces the current in the primary winding by the value of current in secondary winding with factor N_2/N_1. Since the device like current-controlled current source is sometimes differently handled by SPICE-type simulation software, the voltage controlled current source was used instead, and a small resistance of 1 mΩ was added into the secondary winding as current sensor.

Finally, two capacitances C_A and C_B (see fig. 5) were added into the circuit to represent the additional capacitance of the wire to the injection clamp package.

The final circuit representation of the BCI clamp with coupling to a single wire is shown in fig. 5.

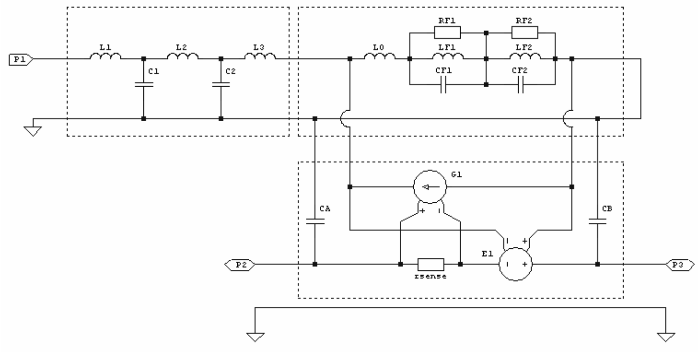

Figure 5. Final equivalent circuit representation of the clamp, including the coupling to a single wire

The wire properties (e.g. self-inductance) are not included in the model. However, when the model of injection clamp is used with a cable model, the necessary properties are introduced with the cable model. The injection clamp model only introduces the changes due to clamping effect. The feedback from the cable to the primary winding will also be modeled correctly.

The model can be extended to multiple wire configurations. The same structure with voltage and current sources must be implemented and the stray capacitances must be added between the wire and probe package.

The resulting model of the injection clamp contains linear components with frequency-independent parameters only, and thus shows good performance in both time and frequency domain simulations.

C. Model verification with long harness

For the purpose of model verification a test setup with 1 m harness was measured and simulated (fig. 6 and 7). A automotive twisted pair cable from Kromberg-Schubert (type “FLRYW”) was used. Accurate models of this cable are available [7].

The cable with length L = 0.3 to 2.0 m was fixed in height H = 50 mm above a metal plane used a ground reference. The both ends of the cable were terminated with 50 Ω ports in grounded metal fixtures. The injected signal levels were measured at these ports with a network analyzer.

The BCI clamp injects the current into all clamped wires simultaneously (common mode). Since the goal of this step was to verify the injection clamp model with a longer harness, the cable wires were soldered together at the terminations and connected to a single port (P2 at left fixture, P3 at right fixture). Thus, pure common mode was forced.

The clamp was located in the middle of the cable, and the exact position was found during the measurement to have the S21 and S31 parameters equal in the entire frequency range. This ensured the symmetry of the setup and avoided the deviations due to clamp misplacement.

Good correlation between model and measurements was observed (fig. 8-10), proving the developed model accuracy.

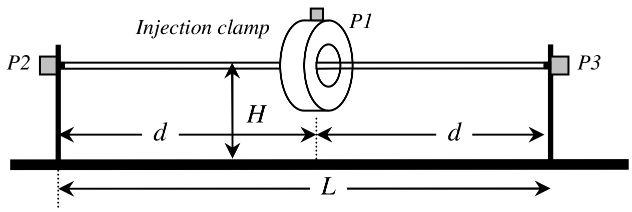

Figure 6. Test setup for BCI injection clamp model verification parameters: L = 1 – 2 m; d = 0.5 L; H = 50 mm.

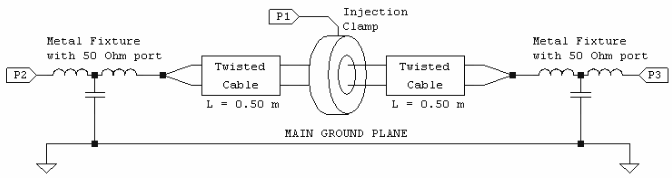

Figure 7. Sketch of verification setup simulation model

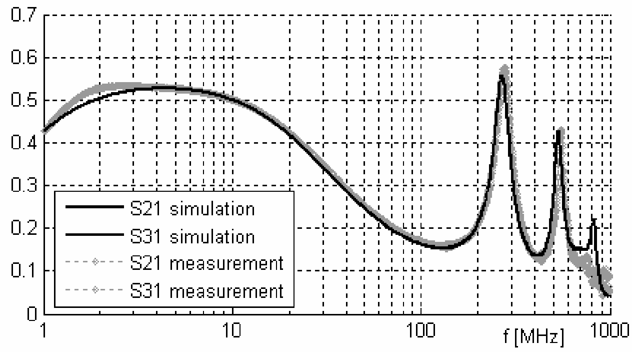

Figure 8. Signal transfer from injection clamp RF port to cable ports

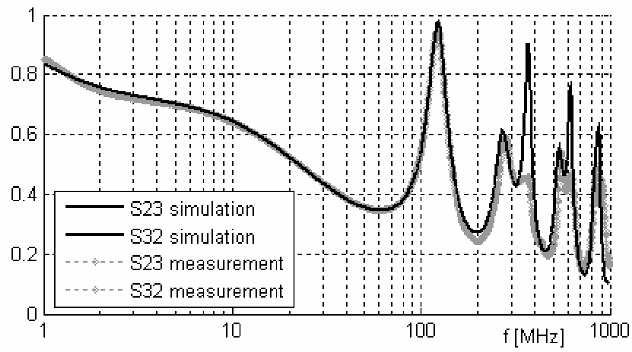

Figure 9. Signal transfer through clamped cable

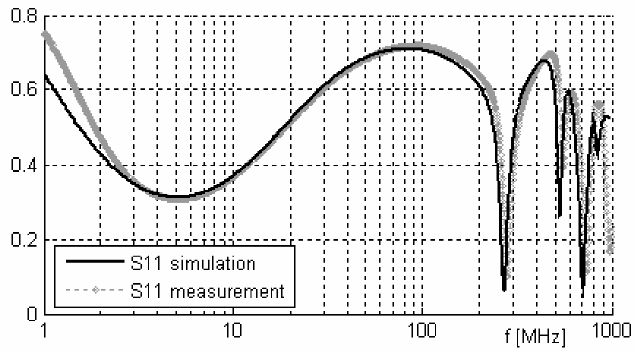

Figure 10. Signal reflection at injection clamp RF port

III. BCI SETUP WITH FLOATING DUT

Many BCI testing specifications require a floating ECU/PCB. In this case the common mode current can flow only through the capacitance between ECU or PCB and ground plane. This setup is very sensitive to small changes and modeling is a challenging task.

A. *Test Setup Description*

When the RF immunity of devices is tested with injection into both power supply and ground cables, there is no explicit connection of the DUT to main ground plane. Such a configuration was measured and modeled (see fig. 11).

A simple resistor of 1 kΩ was used to represent the DUT input impedance. The PCB with the sample DUT was fixed with distance h = 5 to 20 mm from vertical grounded metal plane. The cable was fixed in H = 50 mm from main ground plane. At the supply side of the cable the ground wire was terminated directly into the ground. The power wire was terminated with simple 50 Ω plug, since the standard Artificial Networks have almost 50 Ω impedance in the higher frequency range. At the DUT side the two wires of the cable were connected to power and ground nodes of the PCB correspondingly. The BCI clamp was place in d = 20 cm from dummy DUT.

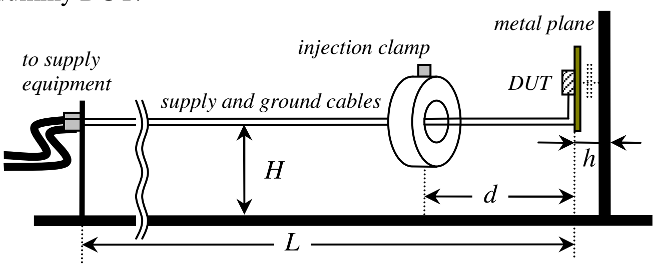

Figure 11. Test setup without direct grounding of PCB

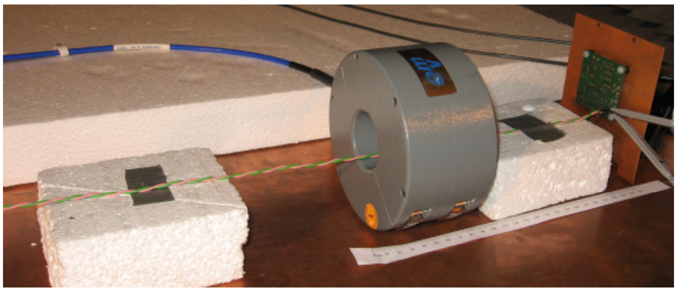

Figure 12. Test setup photo at dummy DUT termination.
Active probes are connected between PCB pins and vertical ground plane.

In this configuration it is difficult to measure the voltage levels on the PCB without affecting the setup. High impedance of the PCB ground plane to main ground plane (C = 5 to 10 pF) is affected especially in higher frequency range by measurement setup. Instead, the current injected into the PCB tracks was measured with a Tektronix CT-6 current sensor.

B. *Floating PCB Impedance to Ground*

The impedance of the floating termination was measured and modeled. 3D simulations with EMCoS EMC Studio software were performed to compute accurately the capacitance. Measurements showed that a capacitance model is not sufficient. A more complex equivalent circuit was necessary to consider the ground plane behaviour.

The impedance of PCB ground to main ground plane was measured with Agilent network analyzer. The measurement has shown the expected mainly capacitive coupling up to approx. 100 or 200 MHz depending on PCB distance to fixture (see fig. 13). To model at higher frequencies a lumped-element circuit shown in fig. 12 was proposed and a curve fitting algorithms in Matlab were used to find the model parameters. The parasitic parameters of VNA port were determined separately and later excluded from the termination model.

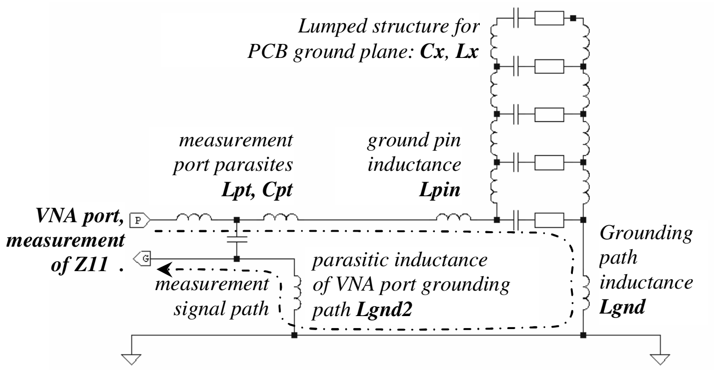

Figure 13. Lumped-element circuit representation of the floating PCB ground plane, including VNA port parasitics and grounding path inductance

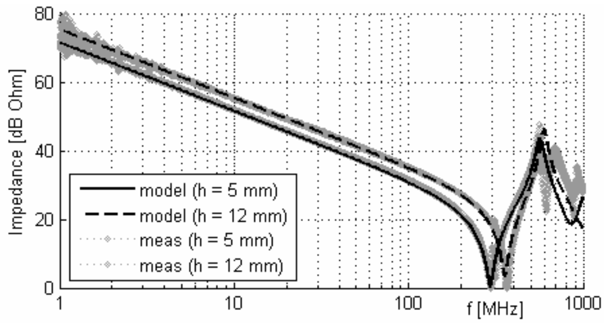

Figure 14. Impedance of PCB ground plane to main ground plane, VNA measurement vs. model, h = 5 and 12 mm

C. *Common Mode Injection*

To verify the model of the floating PCB impedance to ground the common mode injection into this structure was measured and modeled. A simplified setup (see fig. 14) was used for this purpose. The power and ground wires were soldered together at both ends of the cable, thus forcing pure common mode in the line. At the left side the cable was terminated with 50 Ω (VNA port), at the right side cables were connected directly to PCB ground plane. The common mode current in both lines was measured directly at the PCB ground pin with current sensor, terminated with VNA port.

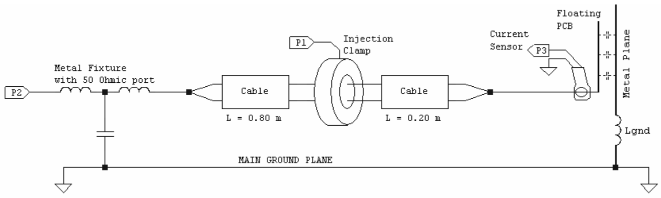

Figure 15. Sketch of simplified common mode setup simulation model

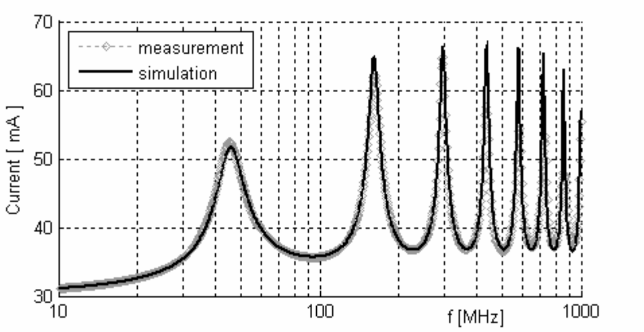

Figure 16. Current into PCB in simplified common mode setup in absense of the injection clamp (P_{FW} = 10 dBm injected into far end of the cable (P2))

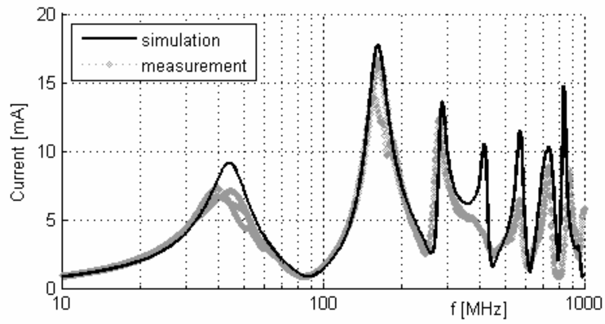

Figure 17. Current injected into PCB in simplified common mode setup (@ P_{FW} = 10 dBm injected into clamp RF port (P1))

With this simplified common mode setup the model gives good results up to 400 MHz (see fig. 16). The results are also acceptable up to 1 GHz, except for the misfit in resonance heights at 400 and 600 MHz. These can be explained by additional losses, probably of radiation origin, which were not yet included in the test setup simulation model.

D. *Common and Differential Mode Injection*

The full setup was assembled as described in section III (A). A resistive load of 1 kΩ was used as input impedance. The BCI injection was performed into both wires.

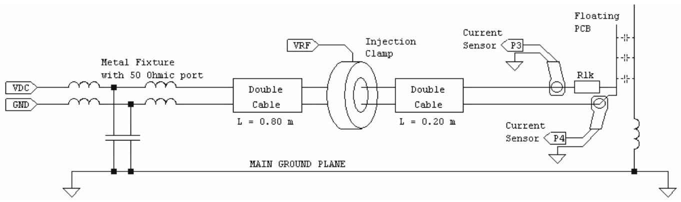

Figure 18. Sketch of the simulation model of the setup with dummy DUT (R = 1 kΩ) on floating PCB

The first measurement was done with a network analyzer. The power of 10 dBm was injected into the BCI clamp, and the currents in DUT power pin and PCB ground pin were measured with current sensors. Taking into account the sensor coupling factor, the current values were restored from S-parameter measurement. The measured and modeled currents are shown in fig. 19.

Using these current values and also the DUT input impedance and PCB impedance to main ground plane, the values of common and differential voltages at the DUT inputs can be calculated.

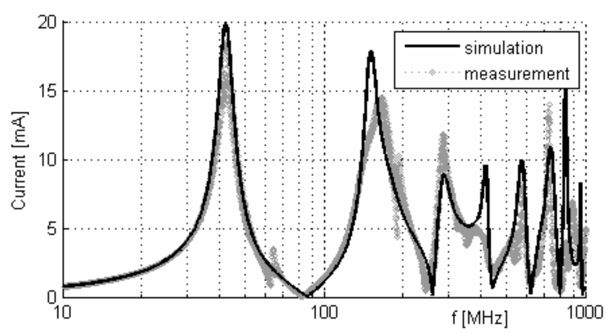

Figure 19. Current into PCB ground plane @ P_{FW} = 10 dBm

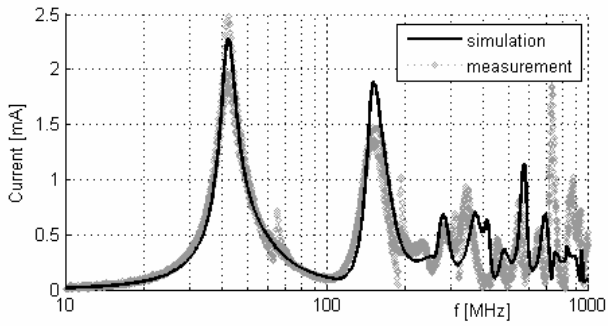

Figure 20. Current into dummy 1 kΩ DUT input pin @ P_{FW} = 10 dBm

The simulation shows acceptable correlation with measurements (fig. 19, 20). In higher frequency range (over 400 MHz) the measurement was disturbed by parasitic couplings on the PCB, (incl. trace inductances and capacitances) which are difficult to model for floating PCB configurations. These effects are not included in the model, but nevertheless the common mode current into PCB ground plane is modeled accurately (fig. 19).

The model was also tested with active probe oscilloscope measurements. RF power of 10 dBm was injected into the clamp, and the signal amplitudes were measured with active probes directly at the PCB power and ground pins relatively to vertical ground plane. Main ground plane could not be used as a measurement reference due to significant distance between measurement points (~ 50 mm), which would add a loop, and thus change the measurement results in higher frequency range. The differential signal was calculated as the difference between signals at power and ground nodes. The influence of the active probes (0.9 pF ‖ 1 MΩ + ~10 nH) was included in the simulation model. The results are shown in fig. 21 and 22.

The injected common mode voltage amplitude, measured with active probes, correlates well with the model in the entire frequency range (see fig. 21). The differential mode disturbance shows good correlation with the model up to 300 MHz (see fig. 22). Due to sensitivity of the setup to external influences and parasitic couplings, the cause of this deviation is not clear. However, in the many applications of such models the exact matching of the resonances is not necessary. It can be sufficient, if the overall level of the injected signal amplitudes is modeled correctly.

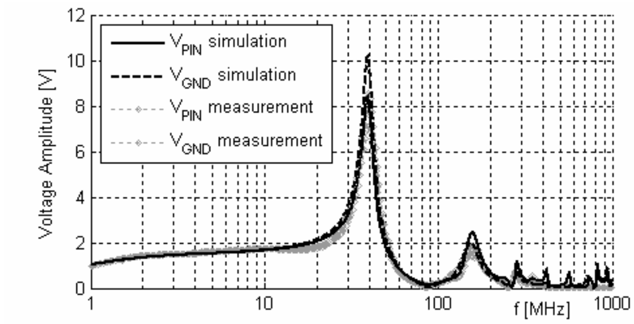

Figure 21. Common mode voltage amplitude at PCB ground plane and DUT input pin relatively to vertical metal plane @ P_{FW} = 10 dBm

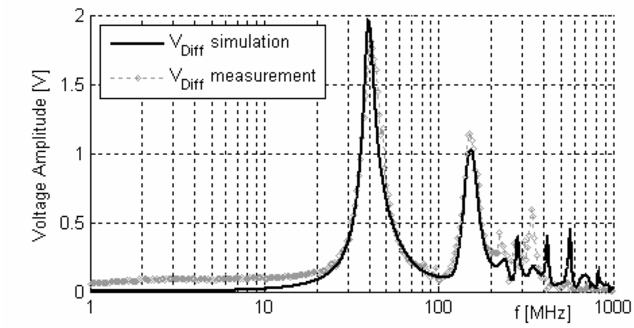

Figure 22. Differential mode voltage amplitude between PCB ground plane and DUT input pin @ P_{FW} = 10 dBm

E. Model application

One of important application of the BCI test setup models is to estimate the RF immunity of developed ECUs in order to be able to perform necessary EMC optimizations. Measuring the RF immunity in several BCI test setup configurations can hardly cover all possible usage scenarios of an IC. Thus, a worst case estimation must be performed.

The test setup with floating DUT is modeled with wide parameter variation. A resistance of 1 k is used instead of the DUT to have a simple input impedance profile. The capacitance of the floating PCB to main ground plane is swept in range from 1.0 to 20 pF representing different sizes of PCBs and distances to ground planes. The length of the cable is varied from 1.0 to 3.0 m, and various positions of the BCI clamp along the cable are modeled.

The simulation is performed according to BCI test standard. The clamp is first calibrated with 50 Ω terminations; the power level corresponding to 50 mA of injected current is recorded as test power limit. During the virtual test the power is increased to obtain 50 mA of injected current, but not higher than the calibrated power value.

The values of injected common and differential voltages are recorded for each parameter set. Then the envelope curves are extracted from simulation data (fig. 23, 24).

The DUT (ECU or another device) can then be investigated with simple RF immunity tests, e.g. in Direct Power Injection (DPI) setup, where the predicted voltage amplitudes can be applied directly to its terminals. If the DUT withstands this type of testing, the probability of passing the customer's BCI tests is significantly increased.

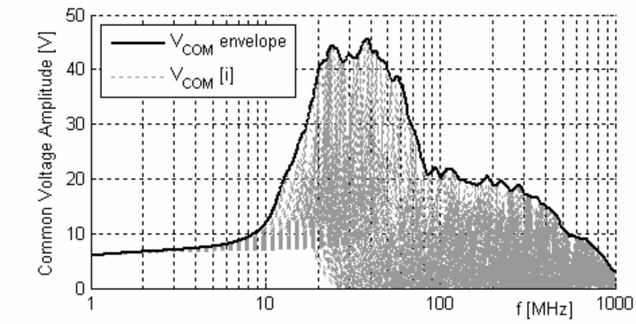

Figure 23. Predicted common mode voltage amplitude in BCI test @ injected current level of 50 mA, limited by clamp calibration

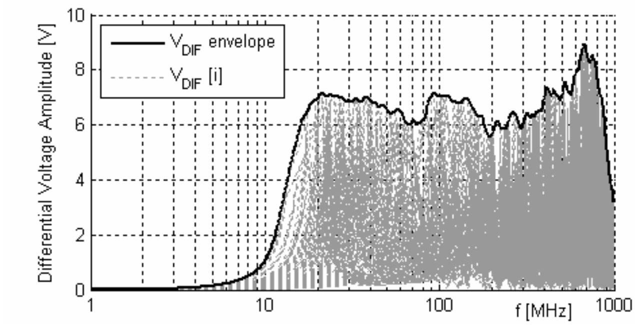

Figure 24. Predicted differential mode voltage amplitude in BCI test @ injected current level of 50 mA, limited by clamp calibration

IV. CONCLUSIONS

A new equivalent circuit model of a BCI injection clamp is proposed. The frequency dependency of the core magnetic permeability is implemented as a linear passive circuit. Usage of complex frequency-domain devices is intentionally avoided. The model is verified within several test setup configurations.

An automotive ECU test setup without explicit grounding of the DUT is modeled and the modeling method is verified by measurements. The impedance of DUT ground path with capacitive coupling to main ground plane is investigated. The common and differential mode voltage amplitudes at DUT pins in BCI test can be predicted with high accuracy.

REFERENCES

[1] ISO 11452-4: Road vehicles – Component test methods for electrical disturbances from narrowband radiated electromagnetic energy, part 4: Bulk current injection (BCI)

[2] IEC 62132-3: Integrated circuits – Measurement of electromagnetic immunity, part 3: Bulk Current Injection (BCI) method.

[3] M. F. Sultan, "Modeling of a bulk current injection setup for susceptibility threshold measurements," IEEE Int. Symp. On Electromagn. Compat. Proceedings, San Diego, CA, 1986, pp. 188-195.

[4] F. Grassi, F. Marliani, S. A. Pignari, "Circuit Modeling of Injection Probes for Bulk Current Injection," IEEE Tran., EMC 49, no. 3, Aug. 2007, pp. 563-576

[5] F. Grassi, F. Marliani, and S. A. Pignari, "SPICE modeling of BCI probes accounting for the frequency-dependent behavior of the ferrite core", in Proc. XIXth General Assembly of U.R.S.I., Chicago, IL, USA, Aug. 7-16, 2008, Commission E, Paper E07.6.

[6] F. Lafon, Y. Belakhouy, and F. De Daran, "Injection probe modeling for bulk current injection test on multiconductor transmission lines," IEEE Symp. on Embedded EMC Proceedings, Rouen, France, 2007.

[7] K. Siebert, H. Günther, S. Frei, W. Mickisch, Modeling of Frequency Dependent Losses of Transmission Lines with VHDL-AMS in Time Domain, EMC Zurich, 2009